COMPUTATION OF A HYDRATION RATE FOR BODIE HILLS OBSIDIAN, FROM MONO COUNTY, EASTERN CALIFORNIA

Alexander K. Rogers, MA, MS
Archaeology Curator
Maturango Museum

June 12, 2013
Rev C

Maturango Museum
Working Manuscript #66C

Abstract

This paper reports a hydration rate for Bodie Hills obsidian from Mono County in Eastern California USA, based on obsidian – radiocarbon pairing data from the western slope of the Sierra Nevada, and on obsidian pairing with temporally-sensitive artifact types from the eastern Sierra. The analysis employs regional temperature scaling to determine site temperature parameters, and temperature-dependent hydration theory to compute hydration rim corrections for effective hydration temperature (EHT), including the effects artifact burial depth. The rate is based on a linear least-squares best fit between the square root of age (independent variable) and EHT-corrected rim value (dependent variable), an algorithm which minimizes errors. The rates determined for the eastern slope and the western slope are statistically indistinguishable when corrected to the same EHT, so the final rate is based on the consolidated data set. The resulting hydration rate is 14.20 ± 0.74 $\mu^2/1000$ yrs at an EHT of 20°C. The rate is valid for both east and west sides of the Sierra Nevada, provided the EHT is computed by the method described herein.

INTRODUCTION

This paper computes a hydration rate for Bodie Hills obsidian, whose source is in Mono County in eastern California, USA. The calculations are based on two sets of data: obsidian-radiocarbon pairing data from the western slope of the Sierra Nevada, kindly provided by Jeff Rosenthal of Far Western Anthropological Research Group (Rosenthal and Waechter 2002); and obsidian pairings with temporally-sensitive artifacts from the eastern Sierra Nevada, kindly supplied by Kirk Halford (Halford 2002). The calculation explicitly takes effective hydration temperature (EHT) into account in computing the rate, using temperature parameters computed from 30-year weather data by regional temperature scaling (Cole 1970; Rogers 2007, 2008a). All EHT values are corrected for burial depth of the artifact. The output is a hydration rate applicable to archaeological sites on either the western or eastern slope of the Sierra Nevada, as long as it is corrected for EHT by the methods described here.

The tentative nature of this rate must be emphasized. The data set employed is relatively error-prone, and an attitude of skepticism is appropriate in applying the rate in chronological analyses until better data are available.

OBSIDIAN MINERALOGY

Obsidian is an alumino-silicate, or rhyolitic, glass, formed by rapid cooling of magma under the proper geologic conditions. Like any other glass, it is not a crystal, and thus it lacks the lattice structure typical of crystals at the atomic level. Glasses do, however possess a matrix-like structure exhibiting some degree of spatial order (Doremus 1994:27, Fig. 2; 2002:59-73). Obsidians are typically about 75% SiO_2 and about 20% Al_2O_3 by weight, the remainder being trace elements, some of which are source-specific (Doremus 2002:109, Table 8.1; Hughes 1988; Stevenson et al. 1998; Zhang et al. 1997). The anhydrous composition of obsidians from a wide variety of sources has been shown to be remarkably consistent (within a few tenths of a weight percent) (Zhang et al. 1997). The minute interstices within the glass matrix, on the order of 0.1 - 0.2 nanometer in diameter, are where water penetration takes place.

All obsidians also contain small amounts of natural water, known as intrinsic water or structural water, resulting from the magma formation process; the amount is generally <2% by weight in natural obsidians, although cases of somewhat higher concentration are occasionally encountered (Zhang et al. 1997). Some of the absorbing water molecules react with atoms of the glass matrix to form hydroxyl (OH^-) groups (Doremus 2002; Silver at al. 1990), so water exists in the obsidian in the form of two species (molecular H_2O and OH^-). However, the hydroxyl reaction does not appear to be significant below the glass transition temperature, ~ 400ºC (Anovitz et al. 2008).

Obsidian anhydrous chemistry, or chemical composition independent of water, has traditionally been regarded as a major influence on hydration rate (see attempts to determine a chemical index to hydration, e.g. in Friedman and Long 1976 or Stevenson and Scheetz 1989). In archaeological analyses, anhydrous chemistry is controlled by grouping and analyzing the obsidian by geochemical source, based on trace element composition as determined by X-ray fluorescence (XRF) or neutron activation analysis. However, Stevenson et al. (1998, 2000) found no consistent influence of anhydrous

chemistry on hydration rate. Zhang and Behrens (2000) and Behrens and Nowak (1997) found the effect of anhydrous chemistry to be negligibly small, although Karsten et al. (1982) reported that Ca^{2+} concentration may influence hydration rate to a very slight extent. It now appears that anhydrous chemistry has negligible effect on hydration rate.

Intrinsic water, on the other hand, has a profound affect on hydration rate (Behrens and Nowak 1997; Delaney and Karsten 1981; Karsten et al. 1982; Lapham et al. 1984; Stevenson et al. 1998, 2000; Zhang et al. 1991; Zhang and Behrens 2000). Four methods are currently used for measuring intrinsic water in obsidian: micro-densitometry (Ambrose and Stevenson 2004); mass loss when obsidian powder is baked (usually called "loss-on-ignition", or LOI) (Newman et al. 1986; Steffen 2005); infrared (IR) transmission spectrometry (Newman et al. 1986); and IR photo-acoustic spectrometry (Stevenson and Novak 2011). Because all these techniques are costly and currently are destructive to the artifact, intrinsic water measurement is not conducted for most practical archaeological investigations in the United States today. The resulting intra-source rate variations increase the uncertainty (statistical error) in age analysis. Operationally, it is likely that controlling for source actually functions as a proxy for controlling for intrinsic water (Stevenson et al. 2000), albeit rather poorly (Stevenson et al. 1993; Rogers 2008b).

THE HYDRATION PROCESS

"Obsidian hydration", in its most basic aspect, simply describes the process by which water is absorbed by obsidian, and involves both physical and chemical changes in the glass (Doremus 2002; Anovitz et al. 2008). (A note on terminology: "adsorption" refers to the process by which water molecules attach themselves to the surface of the glass; "absorption" refers to the transfer of water molecules into the glass matrix; "sorption" refers to the combination of these two processes.) Five steps may be distinguished in the hydration process:

1. When a fresh surface of obsidian is exposed to air, water molecules adsorb on the surface. Since any unannealed obsidian surface exhibits cracks at the nano-scale, the amount of surface area available for adsorption is much greater than the macro-level surface area would suggest, creating a large surface concentration.
2. Some of the adsorbed water molecules, plus others impinging directly from the atmosphere, are absorbed into the glass and diffuse into the interstices in the glass matrix. The diffusion process seems to be driven by three phenomena: a water concentration gradient (Doremus 2002), intra-matrix capillary action (Vesely 2001), and surface tension between the water molecules and the matrix (Vesely 2001, 2008). Although it has been suggested that chemical reactions play a role (Doremus 2002:108ff.; Rogers 2007), it is unlikely that they are a major factor below the glass transition temperature (Anovitz et al. 2008), and thus the "diffusion-reaction" nomenclature of Doremus is likely inappropriate for archaeological temperatures. The glass transition temperature is the temperature at which the glass starts to exhibit fluid-like properties; it is ~400°C, and decreases with increasing water content (Ochs and Lange 1999). Vesiculation tends to occur above the transition temperature (Steffen 2005).

3. The molecules entering the glass by diffusion and by capillary action stretch the glass matrix, causing an increase in volume and openness of the hydrated region. Since the hydrated region is expanded and the non-hydrated region is not, a stress region exists between the two, which can be observed under a polarizing microscope (Scheetz and Stevenson 1988).
4. As time passes, the region of increased water concentration progresses into the glass, its rate being a function of the initial openness of the glass, temperature, and the dynamics of the process itself.
5. When the hydrated layer becomes thick enough, typically greater than 20 microns, the accumulated stresses cause the layer to spall off as perlite (Morgenstein et al. 1999).

MEASUREMENT METHODS

Three general classes of methods have been proposed for measuring obsidian hydration: measurement of water mass uptake or loss vs. time (Ebert et al. 1991; Stevenson and Novak 2011); direct measurement of water profiles vs. depth (Anovitz et al. 1999, 2004, 2008; Riciputi et al. 2002; Stevenson et al. 2004); and observation of the leading edge of the stress zone by optical microscopy (many papers, e.g. Friedman and Smith 1960; Friedman and Long 1979).

Measurement of the mass of water absorbed or lost by an obsidian sample, per unit obsidian mass, is the most physically fundamental method of measuring hydration, and has a long history. Methods employed for such measurements have been mass loss on heating (e.g. Ebert et al. 1991), IR transmission spectrometry (e.g. Newman et al. 1986), and IR photo-acoustic spectrometry (e.g. Stevenson and Novak 2011). It has been shown that mass gain or loss proceeds proportional to t^n where t is time and n is an exponent lying between approximately 0.5 and 0.6 (Stevenson and Novak 2011).

Water profile measurement is generally performed by Secondary Ion Mass Spectrometry (SIMS) or the electron microprobe. The principle is to measure the concentration of H^+ ions, as a proxy for water, as a function of depth. The depth of the half-amplitude point is found to be proportional to t^n, where t is time and n is an exponent lying between approximately 0.6 and 0.7 (Anovitz et al. 1999, 2004; Stevenson et al. 2004; Stevenson and Novak 2011).

The classical field of OHD is based on measuring the position of the stress zone caused by the diffusion process. The stress arises because the volume behind the optical hydration front has enlarged due to penetration of the glass matrix by water molecules, while the matrix of the unhydrated glass has not (Vesely 2001). The stress zone is visible under a polarized microscope due to stress birefringence (Born and Wolf 1908:703-705). Laboratory data (Rogers and Duke 2011; Stevenson and Scheetz 1989; Stevenson et al. 1989; Stevenson et al. 2004) indicate that the position of this stress zone, or hydration front, progresses into the obsidian proportional to t^n, where n is approximately 0.5 within limits of experimental error. Put another way, the position of the hydration front is shown experimentally to progress into the obsidian proportional to the square root of time; the agreement with classical diffusion theory, in particular Fick's formulations and the Boltzmann transformation (Crank 1975:105ff.; Rogers 2007, 2012), may be a

coincidence or may be due to an as-yet-undiscovered property of the hydration process itself.

The present analysis is based on optical measurement of the hydration rim, so the hydration dynamic model employed is

$$r^2 = kt \quad (1)$$

where t is age in calendar years, r is rim thickness in microns, and k is the hydration rate (see e.g. Doremus 1968, 1994, 1999, 2002; Ebert et al. 1991; Rogers 2007, 2012; Stevenson et al. 1989, 1998, 2004; Zhang et al. 1991).

The hydration rate varies with effective hydration temperature (EHT; see e.g. Hull 2001; Onken 2006; Rogers 2007; Stevenson et al. 1989, 1998, 2004), with relative humidity (Friedman et al. 1994; Mazer et al. 1991; Onken 2006), and with intrinsic water concentration in the obsidian (Ambrose and Stevenson 2004; Friedman et al. 1966; Karsten and Delaney 1981; Karsten et al. 1982; Rogers 2008b; Stevenson et al. 1998, 2000; Zhang and Behrens 2000; Zhang et al. 1991). Relative humidity has a small effect in a practical sense, because the interstitial water content of even the driest sand is very high (Friedman et al. 1994), so the effect is generally ignored in practical analyses.

Determining a hydration rate is a problem of parameter optimization, not a regression problem. Regression is a technique to estimate to what extent one variable depends on another. In the present case, however, the degree of dependence is fully known *a priori* from physics and chemistry, so the problem is rather of optimizing a parameter (the rate) which defines the fit between data and the physical model. Mathematically, the formalism used to compute the best fit, described below, is the same as that used in a regression analyses with no linear term and the best-fit line constrained to pass through the origin; the difference is that here the physical model, and hence the degree of dependence, is known.

It follows that, since the form of the hydration equation is known from physics, other forms must be explicitly avoided, such as linear forms or inclusion of higher-order terms or other exponent values. With virtually any archaeological data set it is possible to obtain a better fit (measured by residuals) with MS Excel by other forms of the equation. However, the apparent accuracy thus achieved is spurious, because each data point is a combination of valid data and experimental error, and so a linear or higher degree polynomial or exponent is simply a better fit to the experimental error. If a data set appears to yield a better fit with other functional forms, for example, a linear growth with time (e.g. Bettinger 1989; Meighan 1983), such data can be used to infer a “rule of thumb” correspondence between hydration rim thickness and age for that particular data set, but the resulting parameter is not the “hydration rate” in a strict sense.

Good practice in numerical analysis is to select the model equation based on the nature of the problem (Hanning 1973; Matthews 1992) and then optimize the best fit parameters. For obsidian hydration this means the physical/chemical model, which is a linear dependence of hydration rim thickness on the square root of time.

BODIE HILLS ANALYSIS

The approach taken in this analysis is to infer a hydration rate based on association between obsidian readings and radiocarbon dates or dates inferred from temporally-sensitive artifacts. However, obsidian hydration process is well known to be extremely sensitive to temperature, so it is critical that the obsidian readings all be corrected to a common, known, effective hydration temperature (EHT). This is accomplished by correcting the measured hydration rims by the method of temperature-dependent diffusion theory (Rogers 2007). The necessary temperature parameters are computed from regional temperature scaling (Rogers 2007, 2008a). Once the hydration rim data are reduced to a common EHT they can be combined into a single data set. The radiocarbon ages are all converted to calibrated years before the year 2000 (cyb2k), using the median value of age from Calib 6.0.

The Bodie Hills analysis is based on two data sets. The data set from the western slope of the Sierra Nevada consists of 20 obsidian-radiocarbon pairs from excavations, at elevations ranging from the floor of the Central Valley to CA-CAL-114 at 3444 ft above mean sea level (amsl); see Table 1. The eastern Sierra data (Table 2) consist of temporally-sensitive obsidian projectile points; in most cases elevation is known or can be inferred.

Table 1. Bodie Hills Obsidian-Radiocarbon Pairings, Western Sierra Nevada
(From Rosenthal and Waechter 2002)

Seq. No.	Site	Context	Elevation meters amsl	Age, rcybp	Age std. dev.	median intercept (cal BP)	Rim, μ
1	CAL-991	Component 991A1, 0-20 cm	1005	250	60	300	1.31
2	TUO-2197	Unit 4/5, Feature 3, 30-35 cm	870	270	70	330	2.2
3	Same as #2		870	270	50	340	2.2
4	TUO-407	Unit N104/E97: Feat 6 fill, 20 cm	610	320	110	363	1.9
5	CAL-114/H	Unit 7; Feature 2, 38-73 cm	1050	360	70	400	1.9[2]
6	AMA-56	Feature 1B: 60-76 cm	65	1160	60	1080	3.1
7	CAL-789	Unit S44/W30: 20-50 cm	450	1220	40	1160	3.6
8	CAL-789	Unit S10/E20: 30-40 cm	450	1270	40	1210	3.4
9	PLA-695/H	Unit 95Q: 130-140 cm	670	1340	60	1255	3.8
10	SAC-60	Burial 38-11, 122 cm	2	1550	150	1465	4.0
11	PLA-695/H	Unit 95F: 70-90 cm	670	2170	70	2175	4.5
12	SJO-142	Burial 18, 71 cm	0	2495	120	2560	4.8
13	CAL-789	Feature 1, 60-80 cm	450	2510	40	2580	3.9
14	SJO-68	Burial 23, 120 cm	0	3775	160	4155	4.9
15	SJO-68	Cremation 1, 119 cm	0	4350	250	4950	5.5
16	CAL-629/630	90N/26E, Feat. 232, Black Clay: 203-212 cm	305	8510	150	9050	7.3
17	Same as # 16			8630	145	9370	7.3
18	CAL-629/630	96N/25E, Green Clay, : 225-235 cm	305	9040	90	9990	7.3
19	CAL-629/630	93N/24E, Feat 212, Black Clay: 170-200 cm	305	9230	100	10195	7.4
20	CAL-629/630	86N/23E, Black Clay: 190-200 cm	305	9240	150	10200	8.2

Data for the eastern slope of the Sierra Nevada are based on temporally-sensitive projectile points, since associated radiocarbon data are lacking (Halford 2002). Table 2 shows the point types reported by Halford (2002), with their hydration rim readings and

estimated elevation. The ages are based on Justice (2002), corrected from BC/AD to cyb2k; the standard deviation is the range divided by the square root of twelve.

Table 2. Projectile point data for sites in the eastern Sierra Nevada, from Halford (2002)

Type	N	Rim mean, μ	Rim sd, μ	Elevation, ft amsl	Age range	Mean age, cyb2k	Age sd, yrs
DSN	1	1.3	0.1	7000	AD 1300-1900	400	173
DSN	1	2.8	0.1	6500	AD 1300-1900	400	173
DSN	5	1.82	0.26	6500	AD 1300-1900	400	173
DSN	3	1.4	0.36	8200	AD 1300-1900	400	173
DSN	8	2.05	0.65	6500	AD 1300-1900	400	173
RS/EG	1	3.2	0.1	7000	AD 500 - 1300	1100	231
RS/EG	1	2.8	0.1	6500	AD 500 - 1300	1100	231
RS/EG	7	2.26	0.73	6500	AD 500 - 1300	1100	231
RS/EG	2	2.2	0	8200	AD 500 - 1300	1100	231
RS/EG	4	3.45	0.19	6500	AD 500 - 1300	1100	231
ELK	5	4.5	1.86	7000	1400 BC – AD 650	2375	592
ELK	1	4.8	0.1	6500	1400 BC – AD 650	2375	592
ELK	5	4.84	0.99	8200	1400 BC – AD 650	2375	592
ELK	2	3.65	1.34	6500	1400 BC – AD 650	2375	592
ELK	5	4.28	1.65	6500	1400 BC – AD 650	2375	592
GBS	1	6.4	0.1	8200	9,000 – 6,000 BC	9500	866
GBS	3	5.98	1.5	6500	9,000 – 6,000 BC	9500	866

Correction of the hydration rims to a common EHT requires a temperature analysis, in this case using regional temperature scaling, following the method of Rogers (2007, 2008a). Three temperature parameters are computed from meteorological records: T_a, annual average temperature; V_{a0}, annual temperature variation; and V_{d0}, mean diurnal range. Table 3 presents the temperature parameters for the eastern Sierra, computed from 30-year temperature summaries from the Western Regional Climate Center (WRCC) for seven meteorological stations.

Table 3. Temperature Parameters, East Slope of Sierra Nevada

Station	Alt, ft amsl	T_a, °C	V_a, °C	V_d, °C	EHT, °C
Hawthorn Airport	4220	12.81	23.42	15.75	17.74
Yerington	4380	11.33	22.03	17.64	16.27
Truckee	5980	6.61	18.69	17.81	10.74
Tahoe Airport	6250	6.14	17.03	17.86	9.91
Bridgeport	6370	6.39	19.75	21.19	11.59
Mono Lake	6530	8.28	20.36	15.64	12.36
Bodie	8370	3.28	17.97	21.03	8.02

The resulting temperature scaling equations in °C are

$$T_a = 20.99 - 0.0022h \quad (2a)$$

$$V_{a0} = 27.37 - 0.0012h \quad (2b)$$

$$V_{d0} = 12.24 + 0.001h \quad (2c)$$

Here h is site elevation in ft amsl. The equations were derived from data from 4220 ft amsl to 8370 ft amsl, and should be used with caution for elevations outside this range. Within this elevation range, the equations predict the meteorologically-derived EHT with an error standard deviation of 1.31°C.

The situation is more complex for the western slope, due to temperature inversions in the Central Valley. The inversion layer lies typically at about 1500 ft amsl, and below this there is virtually no variation of temperature parameters with elevation. Table 4 presents the temperature parameters for the western slope, based on WRCC data for twelve meteorological stations.

Table 4. Temperature Parameters, West Slope of Sierra Nevada

Station	Alt, ft amsl	T_a, °C	V_a, °C	V_d, °C	EHT, °C
Sacramento Airport	20	16.19	16.03	13.64	18.94
Stockton	30	16.64	17.31	13.42	19.61
Lodi	40	15.78	15.17	14.44	18.50
Knights Ferry	320	15.50	17.97	14.97	18.89
Electra Power House	700	15.64	16.97	17.69	19.37
New Melones Dam	780	15.47	18.28	16.44	19.22
Auburn	1360	15.72	17.22	12.78	18.57
Sonora	1830	14.36	17.28	17.17	18.04
Placerville	1890	14.47	16.78	15.39	17.69
Grass Valley	2400	12.92	15.50	14.89	15.78
Nevada Cty	2600	12.64	16.50	13.56	15.47
Deer Cr Power House	3700	9.44	17.03	13.75	12.41

The resulting equations for elevations below 1500 ft amsl are

$$T_a = 15.85°C \quad (3a)$$

$$V_{a0} = 16.99°C \quad (3b)$$

$$V_{d0} = 14.77°C \quad (3c)$$

For elevations above 1500 ft amsl, the equations are

$$T_a = 19.44 - 0.0027h \quad (4a)$$

$$V_{a0} = 16.84°C \quad (4b)$$

$$V_{d0} = 14.84°C \quad (4c)$$

Here again h is site elevation in ft amsl. The equations were derived from data from sea level to 3700 ft amsl, and should be used with caution for elevations outside this range. Within this elevation range, the equations predict the meteorologically-derived EHT with an error standard deviation of 0.3°C.

In computing EHT, the temperature parameters at the artifact burial depth are needed, which is related to conditions at the surface by (Carslaw and Jaeger 1959)

$$V_a = V_{a0}\exp(-0.44z) \quad (5a)$$

$$V_d = V_{d0}\exp(-8.5z) \quad (5b)$$

Note that annual average temperature is not affected by burial depth.

The temperature history of each site is modeled by a time series with a sum of three terms: a constant of magnitude T_a, representing annual average temperature; a sinusoid with period of twelve months and amplitude V_a, representing the month-to-month variation of average temperature; and a sinusoid with a period of twenty-four hours and amplitude V_d, representing diurnal temperature variation. The hydration rate is known to depend on temperature by the equation

$$k = k_0 \exp(-E/T) \quad (6)$$

where k is hydration rate, k_0 is a constant, E is the activation energy in °K, and T is temperature in °K (Doremus 2002). The effective hydration temperature is computed from a numerical integration of the hydration rate over the temperature model (see Rogers 2007 for computation details). The computer code to perform the computation is written in MatLab®; copies may be obtained from the author. After determining an EHT for each artifact, based on site elevation and burial depth, a rim correction factor (RCF) is computed to correct the rim value to a consistent reference temperature (EHT_R, chosen as 20°C). The rim correction factor is

$$RCF = \exp\{[-E/(EHT + 273.15)] + [E/(EHT_R + 273.15)]/2\} \quad (8)$$

For small differences in temperatures between EHT and EHT_R, this is roughly equivalent to 6%/°C; however, equation 6 is more accurate for large temperature differences, as in this case. In equation 7, E is the activation energy of the obsidian, typically on the order of 10,000°K (Friedman and Long 1976; Stevenson and Scheetz 1989).

The hydration rate is computed by a linear least-squares best fit between the square root of age and the corresponding hydration rim value. Data points were weighted by the inverse of the variance of the hydration rim reading (Cvetanovic et al. 1979; Meyer 1975). In each case the independent variable (x) is the square root of age, and the dependent variable (y) is the EHT-corrected hydration rim value.

The best-fit slope is computed as (e.g. Cvetanovic et al. 1979; Meyer 1975:71ff)

$$S = \sum w_i N_i x_i y_i / \sum w_i N_i x_i^2 \quad (8)$$

which is the standard best-fit equation for a line constrained to pass through the origin; $\{x_i,y_i\}$ are the data points being fit, each consisting of Ni obsidian-radiocarbon pairs. The parameter wi is a weighting factor defined by

$$wi = 1/\sigma_{yi}^2 \quad (9)$$

where σyi is the standard deviation of the errors in y associated with the i^{th} data point. Since for this case $x = t^{1/2}$ and y = r, equation 8 becomes

$$S = \sum w_i r_i t_i^{1/2} / \sum w_i t_i \quad (10)$$

Using the same data set, the standard deviation of the rate estimate can be computed from

$$\sigma_{ke} = \sigma_r / \sum t_i \quad (11)$$

where

$$\sigma_r^2 = \sum [r_i^2 - S \sqrt{t_i}]^2 \quad (12)$$

(Equation 12 from Taylor 1982:173; equation 13 derived based on Taylor 1982:261, 8.8)

Using the EHT-corrected rim values, and ages derived from either calibrated radiocarbon or temporally-sensitive artifacts, best-fit values of hydration rate were computed for the two data sets. Table 5 shows the resulting rates.

Table 5. Bodie Hills obsidian hydration rates at 20°C.

Statistic	West Slope Data Set	East Slope Data Set
Mean, $\mu/yr^{0.5}$	0.1191	0.1258
Standard deviation, $\mu/yr^{0.5}$	0.0034	0.0177
N	20	4

A t-test for significance gives a t = 0.75, against a threshold value of 1.96 for distinguishability at the 95% confidence level. Thus, the two data sets are not statistically distinguishable and may be merged.

The final rate was thus computed using the merged data sets at an EHT of 20°C, typical of an elevation of 3000 ft in the southern Inyo County. Figure 1 shows the quality of the fit.

The resulting hydration rate is summarized in Table 6. It is shown in two forms for convenience.

Table 6. Bodie Hills obsidian hydration rate.

EHT, °C	Mean Rate	Rate Standard deviation
20	$0.1192\ \mu/yr^{0.5}$	$0.0031\ \mu/yr^{0.5}$
20	$14.20\ \mu^2$/1000 yrs	$0.74\ \mu^2$/1000 yrs

Finally, the age for any set of conditions is

$$t_{cyb2k} = 70.42 \times r_{20}^2 \quad (13)$$

where r_{20} is the hydration rim value corrected to an EHT of 20°C by the methods described above.

DISCUSSION

The hydration rate for Bodie Hills obsidian at 20°C of 14.31 μ^2/1000 yrs is considerably slower than the hydration of Coso obsidians (18.14 μ^2/1000 yrs for West Sugarloaf and 29.87 μ^2/1000 yrs for Sugarloaf Mountain – see Rogers 2013). This slower rate, coupled with the generally lower temperatures typical of high-altitude sites, accounts for the generally small hydration rims encountered in the eastern Sierra Nevada.

To employ this rate the following procedure should be used:

1. Compute temperature parameters for the site from equations 2, 3 or 4, as appropriate. If the site is located in another region, modify the temperature scaling as appropriate. Do not use the Lee equation (Lee 1969).
2. Compute V_a and V_d for the buried artifacts (equation 5).
3. Compute EHT. Numerical integration as described in Rogers 2007 is preferable, but an adequate, although somewhat less accurate, algebraic approximation for EHT is

$$EHT = T_a + 0.0062 \times (V_a^2 + V_d^2). \quad (14)$$

4. Use a reference EHT of 20°C and compute rim correction factors from equation 7.
5. Compute age from equation 14.

The major caveat is that, to employ equation 7, EHT must be computed by the method described herein. The Lee equation (Lee 1969) and various rules of thumb will give incorrect answers.

The rate has an accuracy of approximately 5%, but overall uncertainty in the age estimate is further affected by EHT uncertainties, site formation processes such as turbation, and variability in the intrinsic water of the obsidian source (Rogers 2008b, 2010).

Equation 7 can be used to compute the ages of the specimens from the west side in Table 1, for comparison with the calibrated radiocarbon ages (Figure 2). When this is done, the mean relative error between the model and the radiocarbon data is approximately 5%, showing that the least-squares best fit is eliminating bias quite well. The standard deviation of the percent error is relatively large, 23%; approximately half this error is due to EHT uncertainties, while the remainder probably reflects the poorly-understood chemistry and water content variability of Bodie Hills obsidian (Rogers 2008b).

When applied to the temporally-sensitive point types from the eastern Sierra region, the ages computed for Desert Side-Notched, Rose Spring/Eastgate, and Elko point types generally too large (Figure 2), although the predicted age for Great Basin Stemmed points is 10% too small. The large errors represent the expected uncertainties that arise when trying to estimate a rate based on temporally-sensitive artifacts, since there is no way of knowing when the artifacts were manufactured within long span of time.

Overall, in performing chronometric analyses, it would be unwise to expect an accuracy better than about 20%, given the current state of knowledge of Bodie Hills obsidian.

CONCLUSIONS

The analysis here presents a hydration rate for Bodie Hills obsidian based on obsidian-radiocarbon pairing and on obsidian pairing with temporally-sensitive artifacts. The rate equation as presented in equation 7 is equally valid for east or west sides of the Sierra Nevada, and for surface or buried artifacts, provided the EHT is computed by the method described herein. Accuracy of the age estimate is approximately 20%.

Refinement of hydration rates will require laboratory work to quantify intrinsic water variability, and to develop a lab rate.

ACKNOWLEDGEMENTS

This interesting problem was first brought to my attention by Kirk Halford, former BLM archaeologist at Bishop, California. I thank him for raising the problem and for supplying data from the eastern Sierra Nevada. I also thank Jeff Rosenthal of Far Western Anthropological Research Group for supplying data from the western Sierra Nevada. Above all I thank my wife, Fran, for her patience and encouragement.

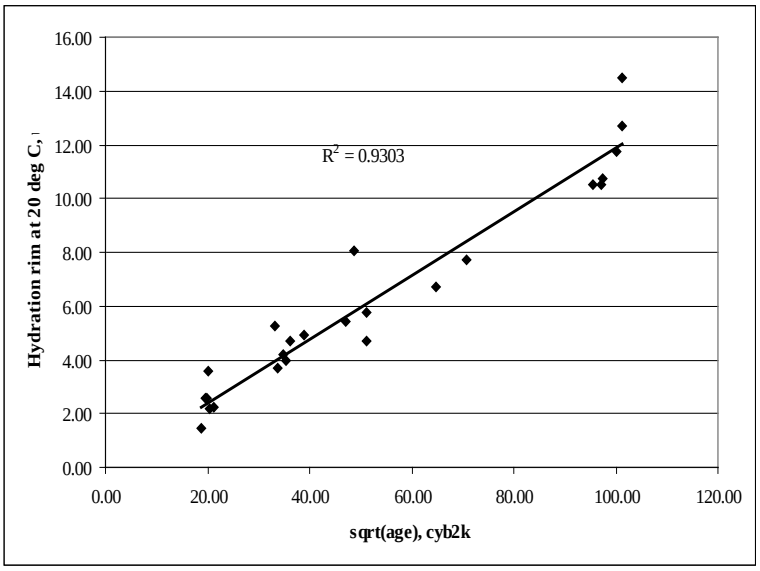

Figure 1. Linear best fit between the square root of calibrated age and EHT-corrected hydration rim values.

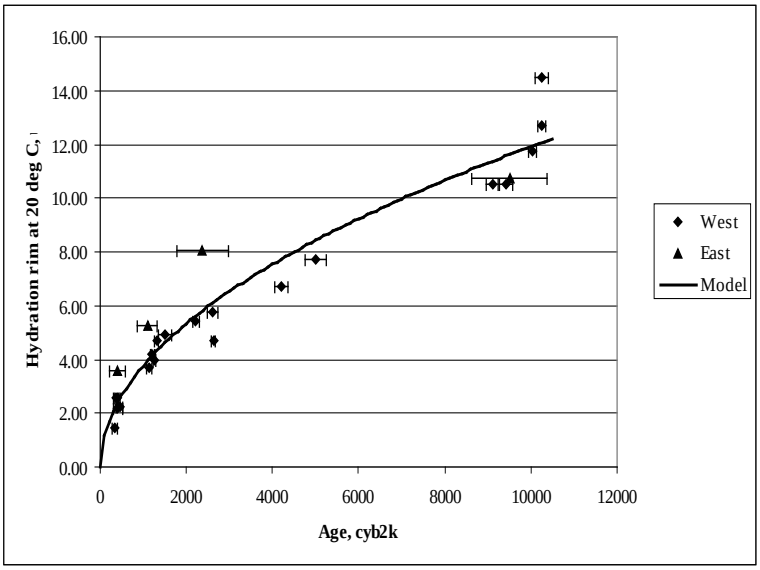

Figure 2. Fit between model and data from sites on the western and eastern slopes of the Sierra Nevada.

REFERENCES CITED

Ambrose, W. R., and C. M Stevenson
2004 Obsidian Density, Connate Water, and Hydration Dating. *Mediterranean Archaeology and Archaeometry* 4(2):5-16.

Anovitz, Lawrence M., J. Michael Elam, Lee R. Riciputi, and David R. Cole
1999 The Failure of Obsidian Hydration Dating: Sources, Implications, and New Directions. *Journal of Archaeological Science* 26(7):735-752.
2004 Isothermal Time-Series Determination of the Rate of Diffusion of Water in Pachuca Obsidian. *Archaeometry* 42(2):301-326.

Anovitz, Lawrence M., David R. Cole, and Mostafa Fayek
2008 Mechanisms of Rhyolitic Glass Hydration Below the Glass Transition. *American Mineralogist* 93:1166-1178.

Behrens, H., and M. Nowak
1997 The Mechanisms of Water Diffusion in Polymerized Silicate Melts. *Contributions to Mineralogy and Petrology* 126:377-385.

Bettinger, Robert L.
1989 Establishing an Hydration Rate for Fish Springs Obsidian. In: *Current Directions in California Obsidian Studies*, Richard E. Hughes, ed., pp. 59-68. Contributions of the University of California Archaeological Research Facility No. 48. University of California: Berkeley.

Born, Max, and Emil Wolf
1980 *Principles of Optics*, 6th ed. Pergamon Press: New York.

Carslaw, H. S., and J. C. Jaeger
1959 *Conduction of Heat in Solids*, 2nd ed. Oxford: Clarendon Press.

Cole, F. W.
1970 *Introduction to Meteorology*. Wiley: New York.

Crank, J.
1975 *The Mathematics of Diffusion*. Oxford: Oxford University Press.

Cvetanovic, R. J., D. L. Singleton, and G. Paraskevopoulos
1979 Evaluations of the Mean Values and Standard Errors of Rate Constants and their Temperature Coefficients. *Journal of Physical Chemistry* 83(1):50-60.

Delaney, J. R., and J. L. Karsten
1981 Ion Microprobe Studies of Water in Silicate Melts: Concentration-Dependent Water Diffusion in Silicon. *Earth and Planetary Science Letters* 52:191-202.

Doremus, R. H.
1968 The Diffusion of Water in Fused Silica, in: *Reactivity of Solids, Proceedings of the 6th International Symposium on the Reactivity of Solids*, J. W. Mitchell, R. C. DeVries, R. W. Roberts, and P. Cannon, eds., pp 667-674. New York: Wiley-Interscience.
1994 *Glass Science*. New York: Wiley Interscience.
1995 Diffusion of Water in Glass. *Journal of Materials Research* 10(9):2379-2389.
1999 Diffusion of Water in Rhyolite Glass: Diffusion-reaction Model. *Journal of Non-Crystalline Solids* 261 (1):101-107.
2002 *Diffusion of Reactive Molecules in Solids and Melts*. New York: Wiley Interscience.

Ebert, W. L., R. F. Hoburg, and J. K. Bates
1991 The Sorption of Water on Obsidian and a Nuclear Waste Glass. *Physics and Chemistry of Glasses* 34(4):133-137.

Friedman, I., and W. D. Long
1976 Hydration Rate of Obsidian. *Science* 191(1):347-352.

Friedman, I., R. I. Smith, and W. D. Long
1966 Hydration of Natural Glass and Formation of Perlite. *Geological Society of America Bulletin* 77:323-328.

Friedman, Irving, and R. Smith
1960 A New Method of Dating Using Obsidian; Part 1, the Development of the Method. *American Antiquity* 25:476-522.

Friedman, I., F. W. Trembour, F. L. Smith, and G. I. Smith
1994 In Obsidian Hydration affected by Relative Humidity? *Quaternary Research* 41(2):185-190.

Halford, F. K.
2002 *New Evidence for Early Holocene Acquisition and Production of Bodie Hills Obsidian*. Paper presented at the 28th Great Basin Anthropological Conference, Elko, NV.

Hanning, R. W.
1973 *Numerical Methods for Scientists and Engineers*. McGraw-Hill: New York.

Hughes, Richard. E.
1988 The Coso Volcanic Field Reexamined: Implications for Obsidian Sourcing and Dating Research. *Geoarchaeology* 3:253-265.

Hull, Kathleen L.

2001 Reasserting the Utility of Obsidian Hydration Dating: A Temperature-Dependent Empirical Approach to Practical Temporal Resolution with Archaeological Obsidians. *Journal of Archaeological Science* 28:1025-1040.

Justice, Noel D.
2002 *Stone Age Spear and Arrow Points of California and the Great Basin.* University of Indiana Press: Bloomington.

Karsten, J. R., and J. L. Delaney
1981. Ion microprobe studies of water in silicate melts: concentration-dependent water diffusion in obsidian. *Earth and Planetary Science Letters* 52: 191-202.

Karsten , J. L., J. R. Holloway, and J. L. Delaney
1982. Ion microprobe studies of water in silicate melts: temperature-dependent water diffusion in obsidian. *Earth and Planetary Science Letters* 59:420-428.

Lapham, K. E., J. R. Holloway, and J. R. Delaney
1984 Diffusion of H_2O and D_2O in Obsidian at Elevated Temperatures and Pressures. *Journal of Non-Crystalline Solids* 67:179-191.

Lee, R.
1969 Chemical Temperature Integration. *Journal of Applied Meteorology* 8:423-430.

Matthews, J. H.
1992 *Numerical Methods for Mathematics, Science, and Engineering*. Prentice-Hall: New York.

Mazer, J. J., C. M. Stevenson, W. L. Ebert, and J. K. Bates
1991 The Experimental Hydration of Obsidian as a Function of Relative Humidity and Temperature. *American Antiquity* 56(3):504-513.

Meighan, C. W.
1983. Obsidian Dating in California: Theory and Practice. *American Antiquity,* 48**,** 600-609.

Meyer, Stuart
1975 *Data Analysis for Scientists and Engineers*. Wiley: New York.

Morgenstein. Maury E, Carolyn L. Wickett, and Aaron Barkett
1999 Considerations of Hydration-rind Dating of Glass Artefacts: Alteration Morphologies and Experimental Evidence of Hydrogeochemical Soil-zone Pore Water Control. *Journal of Archaeological Science* 26:1193-1210.

Newman, S., E. M. Stolper, and S. Epstein
1986 Measurement of Water in Rhyolitic Glasses: Calibration of an Infrared Spectroscopic Technique. *American Mineralogist* 71:1527-1541.

Ochs, Frederick A., and Rebecca A. Lange
1999 The Density of Hydrous Magmatic Fluids. *Science* 283:1314-1317.

Onken, Jill
2006 *Effective Hydration Temperature and Relative Humidity Variation within the Nevada Test and Training Range, Southern Nevada*. Statistical Research Inc. Technical Report 06-50.

Riciputi, Lee R., J. M. Elam, L. M. Anovitz, and D. R. Cole
2002 Obsidian Diffusion Dating by Secondary Ion Mass Spectrometry: A Test Using Results from Mound 65, Clalco, Mexico. *Journal of Archaeological Scienc*e 29:1055-1075.

Rogers, Alexander K.
2007 Effective Hydration Temperature of Obsidian: A Diffusion-Theory Analysis of Time-Dependent Hydration Rates. *Journal of Archaeological Science* 34:656-665.
2008a Regional Scaling for Obsidian Hydration Temperature Correction. *Bulletin of the International Association for Obsidian Studies No. 39*, Summer 2008, pp. 15-23.
2008b Obsidian Hydration Dating: Accuracy and Resolution Limitations Imposed by Intrinsic Water Variability. *Journal of Archaeological Science*. 35:2009-2016.
2010 Accuracy of Obsidian Hydration Dating based on Obsidian-Radiocarbon Association and Optical Microscopy. *Journal of Archaeological Science* 37:3239-3246.
2012 Temperature Correction for Obsidian Hydration Dating, pp. 46-56. In: *Obsidian and Ancient Manufactured Glasses*, Ioannis Liritzis and Christopher Stevenson, eds. University Of New Mexico Press: Albuquerque.
2013 *Flow-Specific Hydration Rates for Coso Obsidian*. Proceedings of the Society for California Archaeology, vol. 27 (in press)

Rogers, Alexander K., and Daron Duke.
2011 An Archaeologically Validated Protocol for Computing Obsidian Hydration Rates from Laboratory Data. *Journal of Archaeological Science* 38:1340-1345.

Rosenthal, Jeffrey S. and Sharon A. Waechter
2002 *Results of Phase-II Test Excavations at CA-ELD-616/H near Cool, Western El Dorado County.* Report prepared for CalTrans District 03,

Marysville, California.

Scheetz, Barry E., and Christopher M Stevenson
1988 The Role of Resolution and Sample Preparation in Hydration Rim Measurement: Implications for Experimentally-determined Hydration Rates. *American Antiquity* 53(1):110-117.

Silver, L. A., E. M. Ihinger, and E. Stolper
1990 The Influence of Bulk Composition on the Speciation of Water in Silicate Glasses", *Contributions to Mineralogy and Petrology* 104:142-162.

Steffen, Anastasia
2005 *The Dome Fire Obsidian Study: Investigating the Interaction of Heat, Hydration, and Glass Geochemistry*. PhD dissertation, University of New Mexico.

Stevens, Nathan E.
2005 Changes in Prehistoric Land Use in the Alpine Sierra Nevada: A Regional Exploration using Temperature-Adjusted Obsidian Hydration Rates. *Journal of California and Great Basin Anthropology* 25(2):41-59.

Stevenson, C. M., and B. E. Scheetz
1989 Induced Hydration Rate Development of Obsidians from the Coso Volcanic Field: A Comparison of Experimental Procedures. In: *Current Directions in California Obsidian Studies*, Richard E. Hughes. ed., pp. 23-30. Berkeley: Contributions of the University of California Archaeological Research Facility No. 48.

Stevenson, C. M., J. Carpenter, and B. E. Scheetz
1989 Obsidian Dating: Recent Advances in the Experimental Determination and Application of Hydration Rates. *Archaeometry* 31(2):1193-1206.

Stevenson, C. M., E. Knauss, J. J. Mazer, and J. K. Bates
1993 The Homogeneity of Water Content in Obsidian from the Coso Volcanic Field: Implications for Obsidian Hydration Dating. *Geoarchaeology* 8(5):371-384.

Stevenson, C. M., J. J. Mazer, and B. E. Scheetz
1998 Laboratory Obsidian Hydration Rates: Theory, Method, and Application. In: *Archaeological Obsidian Studies: Method and Theory. Advances in Archaeological and Museum Science*, Vol. 3, M. S. Shackley, ed., pp.181-204. New York: Plenum Press.

Stevenson, C. M., M. Gottesman, and M. Macko
2000 Redefining the Working Assumptions for Obsidian Hydration Dating. *Journal of California and Great Basin Anthropology* 22(2):223-236.

Stevenson, C. M., I. M. Abdelrehim, and S. W. Novak
2004 High Precision Measurement of Obsidian Hydration Layers on Artifacts from the Hopewell Site Using Secondary Ion Mass Spectrometry. *American Antiquity* 69(4):555-568.

Stevenson, Christopher M., and Steven W. Novak
2011 Obsidian Hydration Dating by Infrared Spectroscopy: Method and Calibration. *Journal of Archaeological Science* 38:1716-1726.

Taylor, John R.
1982 *An Introduction to Error Analysis.* Mill Valley: University Science Books.

Vesely, D.
2001 Molecular Sorption Mechanism on Solvent Diffusion in Polymers. *Polymer* 42:4417-4422.
2008 Diffusion of Liquids in Polymers. *International Materials Reviews* 53(3):299-315.

Zhang, Y., and H. Behrens
2000 H_2O Diffusion in Rhyolitic Melts and Glasses. *Chemical Geology* 69:243-262.

Zhang, Y., E. M. Stolper, and G. J. Wasserburg
1991 Diffusion of Water in Rhyolytic Glasses. *Geochimica et Cosmochimica Acta* 55:441-456.

Zhang, Youxue, R. Belcher, P. D. Ihinger, Liping Wang, Zhengjiu Xu, and S. Newman
1997 New Calibration of Infrared Measurement of Dissolved Water in Rhyolytic Glasses. *Geochimica et Cosmochimica Acta* 61(15:2089-3100)